Synthesis and Characterization of Biodegradable, Photocuring Elastomers for Soft Robotics Applications

By
Jacob Rueben

A THESIS

submitted to

Oregon State University

University Honors College

in partial fulfillment of
the requirements for the
degree of

Honors Baccalaureate of Science in Chemical Engineering
(Honors Scholar)

Presented June 01, 2017
Commencement June 2017

AN ABSTRACT OF THE THESIS OF

Jacob Rueben for the degree of Honors Baccalaureate of Science in Chemical Engineering presented on June 01, 2017. Title: Synthesis and Characterization of Biodegradable, Photocuring Elastomers for Soft Robotics Applications

Abstract approved:

Yigit Menguc

This work introduces a safe, UV-curing, biodegradable, renewable elastomer, poly(glycerol sebacate itaconate), or PGSI, for use in soft robotics. A simple synthesis route using safe and inexpensive chemical reagents was developed to enable easy adoption into soft robotics labs. The biodegradable nature of PGSI enables its use in disposable robots, or robots that do not need to be retrieved after use. Material characterization of non-aged PGSI samples gave: ultimate tensile strength ranging from 134 to 193 kPa with moduli ranging from 57 to 131 kPa and elongations at break ranging from 105 to 137 % (12 samples from 6 batches tested), and resilience values ranging from 73 to 82 % (3 samples from 3 batches tested). Fourier-Transform Infrared Spectroscopy showed a possible decrease in carbon-carbon double bonds after UV curing, evidencing a decrease in itaconic acid methylene groups from photoinitiated free radical cross-linking.

Key Words: Green Materials, Soft Robotics, Biodegradable Materials

Corresponding e-mail address: ruebenj@oregonstate.edu

Synthesis and Characterization of Biodegradable, Photocuring Elastomers for Soft Robotics Applications

By
Jacob Rueben

A THESIS

submitted to

Oregon State University

University Honors College

in partial fulfillment of
the requirements for the
degree of

Honors Baccalaureate of Science in Chemical Engineering
(Honors Scholar)

Presented June 01, 2017
Commencement June 2017

Honors Baccalaureate of Science in Chemical Engineering project of Jacob Rueben presented on June 01, 2017

APPROVED:

Yigit Menguc, Mentor, representing Mechanical, Industrial and Manufacturing Engineering

---

John Simonsen, Committee Member, representing Wood Science & Engineering

---

Steph Walker, Committee Member, representing Mechanical, Industrial and Manufacturing Engineering

---

Toni Doolen, Dean, Oregon State University Honors College

I understand that my project will become part of the permanent collection of Oregon State University Honors College. My signature below authorizes release of my project to any reader upon request.

Jacob Rueben, Author

Contents

1 Introduction

Soft materials are applied in the field of soft robotics, which uses them to generate vastly different motion profiles than existing stiff robots (Rus and Tolley, 2015). Unlike traditional, stiff robots, soft robots derive much of their actuation by taking advantage of the properties of their materials of construction, which are often elastic materials (Cho et al., 2009). For example, pneumatically actuated soft robots are usually made either partially or fully of elastic polymers. Many of these elastomeric materials are either non-biodegradable or made from non-renewable feedstocks. Silicone rubbers, for example, do not readily biodegrade and are created through an irreversible cross-linking process (Dow Corning, 2016, Lukasiak et al., 2005). The use of silicones and other non-green materials result in soft robots that are often dependent on depleting resources, are not re-processable, and are limited to disposal in landfills.

Biodegradable and renewable elastomeric materials have recently become a larger area of interest, due to their applications in medicine (Yang et al., 2004, Zhao et al., 2015), and more recently, soft robotics (Walker et al., 2017). Many biodegradable elastomers have been created and documented, but are either not made from renewable materials or are difficult to manufacture in geometries required for soft robotic applications. A recently synthesized photocurable elastomer, poly(glycerol sebacate) acrylate (Nijst et al., 2007), would possibly enable stereolithography as a method of actuator manufacturing. However, the acryloyl chloride used to acrylate the PGS

is non-renewable and harmful to human and environmental health (Sigma-Aldrich, 2016). Its synthesis method is also complex and requires equipment not easily obtained or operated by conventional roboticists—a common theme resulting in a perceived rift between the fields of materials science and robotics (Nijst et al., 2007, Wang et al., 2002, Daemi et al., 2016). Thus, there exists a need for a biodegradable, green, elastic polymer with simple and favorable manufacturing options for use in soft robotic actuator construction.

In this work we propose a UV-curable, biodegradable, and renewable elastic polymer for use in soft robotics, poly(glycerol sebacate itaconate), or PGSI. The synthesis route was kept facile and most equipment was constructed of easily accessible parts, in an attempt to make the synthesis adoptable by robotics labs.

2 Background and related works

2.1 Soft Robotics

Soft robotics is an emerging field that utilizes soft materials to produce motion paths difficult to obtain with stiff robots (Rus and Tolley, 2015). Soft robots are often biologically inspired, due to the many soft actuation analogues found in marine life and terrestrial non-skeletal systems (Ilievski et al., 2011). The octopus, jellyfish, amoeba, and worm are all examples of biological systems that have inspired soft robot designs (Laschi et al., 2012, Godaba et al., 2016, Leon-Rodriguez et al., 2015,

Seok et al., 2013). Soft robots have many applications, including handling fragile objects and moving over uneven or unpredictable terrain (Ilievski et al., 2011). Soft robots can also be capable of continuous deformation without needing complex joints (Shian et al., 2015). This allows the output of non-linear motion paths from simple inputs, giving them an advantage over stiff robots (Mosadegh et al., 2014).

Soft robots can actuate via chemical, electrical, and pneumatic (gas pressure-driven) methods, among others. Soft pneumatic actuators (SPAs) are particularly popular due in part to their low cost and easy assembly (Agarwal et al., 2016). SPAs are commonly assembled from elastic materials such as silicone rubbers (Moseley et al., 2016), and can achieve linear extension, contraction, bending, and rotation motion profiles through selective inflation and deflation of one or more elastic cavities (Agarwal et al., 2016).

The complex actuation paths of pneumatic soft robots result from leveraging material properties to produce motion. Because of this, two SPAs of identical size and shape but different material composition and construction can produce drastically different motion paths (Connolly et al., 2015). Therefore, both material choice and construction are pivotal factors in designing a pneumatic soft robot. While inelastic materials can be used in soft robots (Miyashita et al., 2015), SPAs rely mainly on elastic materials to move via inflation. Due to this, the field of elastic materials research is directly tied to the capabilities of SPAs.

2.2 Elastomers

Elastomers, or elastic polymers, are a class of material commonly used in soft robots (Ilievski et al., 2011). When choosing elastomers for use in an SPA, several criteria must be met. First of all, the material must be compliant within a pressure range achievable by the designed system. Typically, soft robots use materials with Young's moduli between 10^4 and 10^9 Pa to fulfill this prerequisite (Rus and Tolley, 2015). Elastomers for use in SPAs can be created via techniques like additive manufacturing, injection molding, or individual layer adhesion.

Arguably the most commonly used polymers in soft robots are silicones, which are comprised of an alternating silicon-oxygen backbone. Silicones can be cured into elastomers (called silicone rubbers) by multiple methods, including condensation (curing in the presence of moisture) and by addition cross-linking, the latter often being catalyzed by platinum or rhodium metal complexes (Colas and Aguadisch, 1997). Many silicone curing systems can be acheived at standard temperature and pressure, making SPA assembly a relatively simple endeavor. Silicone rubbers also have the advantage of being commercially available in various chemistries, providing a wide range of curing times and material properties (Lorenz and Kandelbauer, 2014). While silicone rubbers are well-suited to SPA construction, they are not entirely environmentally friendly. Some silicones are chemically degradable, but many others are chemically inert (Walker et al., 2017). This lack of degradability, bio-driven or otherwise, can lead to a sizable impact on the environment (Lukasiak et al., 2005). This contributes to

the importance of applying the principles of green chemistry to soft robotics research.

2.3 Green Materials

Green chemistry is the reduction or elimination of hazardous feedstocks and emissions though aimed design of chemical processes and products (Anastas and Eghbali, 2009). Attempts at applying green chemistry to the plastics industry have resulted in research into two types of green polymers: biodegradable polymers and biobased polymers. Biodegradable polymers undergo a thermochemical process to degrade into CO_2, water, and biomass in a defined time frame and disposal environment. Biobased polymers, on the other hand, are polymers composed partially or entirely of biological products or renewable agricultural material (Greene, 2014). Put simply, the term biobased refers to the feedstock of the polymer, while the term biodegradable refers to the polymer's lifespan.

Biodegradable and biobased elastomers have been of increasing academic interest over the past two decades. Biodegradable polymers of interest include natural rubber, poly(1,8-octanediol-*co*-citric acid) (Yang et al., 2004), alginate-based supramolecular ionic polyurethanes (ASPUs) (Daemi et al., 2016), and poly(glycerol sebacate) (Wang et al., 2002). Of these materials, many rely on nonrenewable feedstocks, keeping the materials from being fully biobased. Poly(glycerol sebacate), or PGS, was determined to have the most potential as a green alternative to silicone rubbers in SPA manufacturing due to its biodegradable nature, its use of biobased feedstocks, its relatively

safe and simple synthesis process, and its favorable mechanical properties (Walker et al., 2017, Wang et al., 2002).

2.4 Cross-Linking

As previously mentioned, ease of assembly is a main criterion for a material being used in soft robot construction. While many conventional materials have simple metrics such as melting point to convey the environment in which it can be processed, thermoset elastomers are more complicated. Unlike thermoplastics, thermally setting elastomers can undergo an irreversible curing process called chemical cross-linking. In this step, linear or branched polymers (often called the pre-polymer) are chemically and permanently bonded to each other to form a network polymer. These newly-formed chemical bonds are referred to as cross-links, and affect the final mechanical properties of elastomers (Dodiuk and Goodman, 2014).

Multiple types of cross-linking polymers exist, one form being thermosets, which chemically cross-links with inputted thermal energy. The resulting material is infusible and insoluble (Ratna, 2009). PGS is an example of a thermoset, as it requires a lengthy curing time in a vacuum oven (Wang et al., 2002). Using thermoset elastomers as an SPA building material proves a difficult task, due to the materials' incompatibility with conventional room-temperature SPA manufacturing methods, such as 3D printing. Functioning SPAs have been made out of a thermosetting PGS, but the possible structures were limited by the method of assembly (gluing together

shapes cut out of PGS sheets) (Walker et al., 2017). These limitations make thermoset elastomers an inconvenient material for SPA construction.

A curing method more compatible with SPA assembly is ultraviolet (UV) curing. UV curing usually works alongside a photoinitiator, which is added to the uncured pre-polymer. The photoinitiator works by absorbing UV light to create a reactive species, which interacts with the pre-polymer to begin a polymerization reaction (Green, 2010). This polymerization reaction is called a photopolymerization due to its light-induced initiation (Fouassier and Lalevée, 2012). Due to their ability to be cured at room temperature, photopolymers have already been applied in commercial additive manufacturing products by companies such as Formlabs and Stratasys (Formlabs, 2017, Stratasys, 2017).

PGS has already been modified to make a photocurable elastomer, called poly(glycerol sebacate) acrylate, or PGSA (Nijst et al., 2007). The added acrylate groups provide a point of unsaturation (a carbon-carbon double bond) with which a free-radical photoinitiator can react (Mucci and Vallo, 2012). However, PGSA uses acryloyl chloride, an acutely toxic chemical that can cause death if inhaled, to add these acrylate groups (Sigma-Aldrich, 2016). Itaconic acid, a weak organic acid obtained from distillation of glucose, has been used to make photocurable and biodegradable polyesters (Magalhães et al., 2017, Barrett et al., 2010). Itaconic acid is a dicarboxylic acid, making it compatible with the polycondensation reaction of PGS formation, potentially taking the place of sebacic acid in the polymer backbone. Itaconic acid's

terminal methylene group provides a point of unsaturation, making it compatible with free-radical photoinitiators. To try to make a greener, biobased, biodegradable, and UV-curing elastomer for use in SPA assembly, we added itaconic acid to PGS chains to make it compatible with commercial free-radical photoinitiators. We utilized 1-hydroxycyclohexyl phenyl ketone (HCHPK) as a free-readical photoinitiator due to its common usage, its low health risk, its 80% biodegradability, and its attainable activation wavelength range of approximately 220 to 300 nm (Li et al., 2017, Sigma-Aldrich, 2014, Ciba Specialty Chemicals, 2001).

3 Materials and methods

3.1 Construction of UV-curing chamber

Two 15 W UV CFL bulbs with 254 nm wavelength (LSE Lighting) were secured to the inside of a cardboard file storage box, and wired to two pendant lamp cords with in-line switches. The inside of the box was coated with aluminum foil, and a flap was cut to serve as a door. A blackout cloth was also purchased to place over the entire UV-curing assembly to prevent any incident UV radiation from escaping. Three acrylic stands were assembled to hold a sample between the two bulbs and at roughly equal distances from said bulbs, such that samples could be cured from both the top and bottom simultaneously. The UV-curing chamber is shown in Figure 1.

Figure 1: Inside of UV-curing chamber, built as specified in Section 3.1. Dumbbell mold (Section 3.2) is also pictured.

3.2 Construction of dumbbell mold

A tempered borosilicate glass 3D printing plate (Signstek via Amazon, 213 mm by 200 mm by 3 mm) was used as the bottom layer of the dumbbell mold, due to the high UV transmission of borosilicate glass compared to soda lime glass and clear acrylic (QVF Group, 2007). A sheet of clear acrylic was then cut to fit four dumbbells with all dimensions except for thickness specified by ASTM D412 for Die C (height 25 mm $\pm$ 1 mm, width 115 mm minimum, gauge length 33 mm $\pm$ 2 mm, gauge width 6 mm $+$ 0.05 mm, large curvature radius 25 mm $\pm$ 2 mm, small curvature radius 14 mm $\pm$ 1 mm) (ASTM International, 2016). The acrylic sheet with dumbbell cut-outs was then adhered to the borosilicate glass sheet with cyanoacrylate liquid glue (Loctite Super Glue Liquid Professional). Once dry, excess glue was scraped off of the exposed

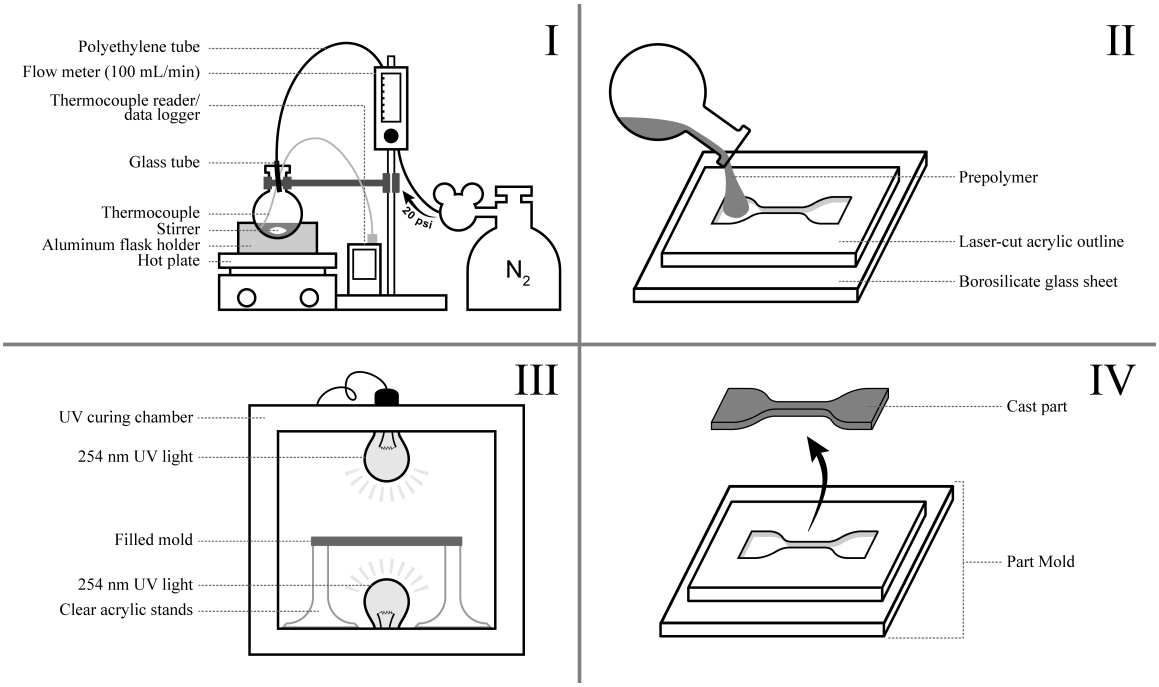

Figure 2: Synthesis of a PGSI part involves a melt process **(I)**, followed by the pouring of prepolymer into a UV-transmissive mold **(II)**, a curing process in a UV-curing chamber **(III)**, and removal of part from mold **(IV)**.

glass in the dumbbell-shaped cavities with a razor blade.

3.3 Synthesis of PGSI

Glycerol (Fisher Scientific) and sebacic acid (Sigma-Aldrich, 99%) were melted in a 0.16:0.195 molar ratio with a target temperature range of 135 to 140°C in a 250-ml round-bottom flask for 20 hours under approximately 100 ml/min nitrogen flow. Mixing was maintained with a magnetic stir bar, with the hot plate (IKA C-Mag HS 7) set at level 1 mixing. After 20 hours, itaconic acid (Sigma-Aldrich, 99%) was added to the heated flask in a 0.035:0.16 molar ratio to sebacic acid. After three more hours, or 23 hours after trial initiation, HCHPK (Sigma-Aldrich, 99%) was added to

the heated flask such that it was 0.89 wt% of the final melt (pre-polymer). The flask was removed from heat after 24 hours had passed since trial initiation.

The pre-polymer was then poured into the dumbbell mold, previously prepared with a silicone-based mold release spray (Farwest Materials Ease Release® 200), and the top of each filled cavity was scraped with a putty knife to ensure even sample thicknesses. The filled mold was left to cool at room temperature for approximately 15 minutes before being placed in the UV-curing chamber on top of acrylic stands, between the two bulbs. The chamber was then shut, the blackout cloth was placed on top of the chamber, and the two bulbs were turned on. The mold was left to cure for 30 minutes, rotated 180 degrees to ensure even curing between dumbbells, and cured for another 30 minutes. The filled mold was then removed from the chamber and left to cool in darkness until at room temperature. Each dumbbell was then carefully removed from the mold so as to not pre-stretch the samples, and placed on a teflon baking sheet (Linden Sweden via Amazon) for storage. This whole process is illustrated in Figure 2.

3.4 Tensile and cyclic testing

Tensile testing was performed on molded sample dumbbells using a Mark-10 Tensile Tester (22 N load cell) with an extension rate of 500 mm/min as specified by ASTM D412 (ASTM International, 2016). Four dumbbells were synthesized per run as specified in Section 3.3, with two of each batch tested on day 0 with the specified

tensile testing parameters. Modulus curves were calculated by fitting fourth-degree polynomials to the stress-elongation curves, then taking the derivative of the fitted polynomial with respect to strain. Modulus values were calculated by taking the average of the modulus curves in the range of 0 to 10 % elongation. This resultant modulus curve was plotted against elongation % and compared to Smooth-On Ecoflex® 00-30 (a platinum-cure silicone commonly used in soft robot construction). One of the remaining two dumbbells was tested with the same tensile testing parameters after 7 days of aging in darkness at room temperature.

The final dumbbell from each batch was run through cyclic testing, which was also performed on the Mark-10 Tensile Tester (22 N load cell). The extension rate was set to 500 mm/min. Each sample was pulled to one third of the average elongation at break of the two tensile tested dumbbells from the same batch for up to 100 cycles. Hysteresis behavior was analyzed via a stress vs. % elongation plot. The resilience (percent of energy retained by sample) was calculated using cycle 100 data, or the last full cycle before break if the sample broke during testing. To find the resilience, the areas under the loading curve and unloading curve (A_L and A_U, respectively) were used (Equation 1) (Bellingham et al., 2003).

$$Resilience\ \% = 1 - \frac{A_L - A_U}{A_L} \tag{1}$$

3.5 Pocket actuator assembly

Pocket actuators were assembled out of PGSI with a mold of similar construction to that in Section 3.2. The mold cavity was a cylinder 34 mm in diameter and approximately 4.5 mm in depth. Silicone mold release was sprayed on empty mold prior to filling. A layer approximately 2 mm in thickness of PGSI prepolymer was poured into the mold. A 25 mm diameter circle of colored printer paper was cut, with another hole of 2 mm diameter in the center, to make an annulus (see Figure 3-III). A 4 mm outer diameter latex tube was glued to the paper annulus such that the latex tube hole aligns with the paper's 2 mm hole. The paper-tubing assembly was placed paper-down on top of the poured layer of PGSI pre-polymer, and covered with more pre-polymer until the mold was filled. The filled mold was then cured using the assembly described in Section 3.1 and shown in Figure 1 for 2 hours before removal, the mold rotated halfway through curing. Cure time was longer for pocket actuators than for dumbbells due to increased part thickness.

The actuators were then removed from the mold, and any gaps around the latex tube at the PGSI surface were sealed with cyanoacrylate glue. The actuators were inflated slowly with air to separate the bottom layer from the paper.

3.6 FTIR Analysis

Fourier-Transform Infrared Spectroscopy (FTIR) was performed on the prepolymer and cured dumbbells in attenuated total reflectance (ATR) mode using a Nicolet™

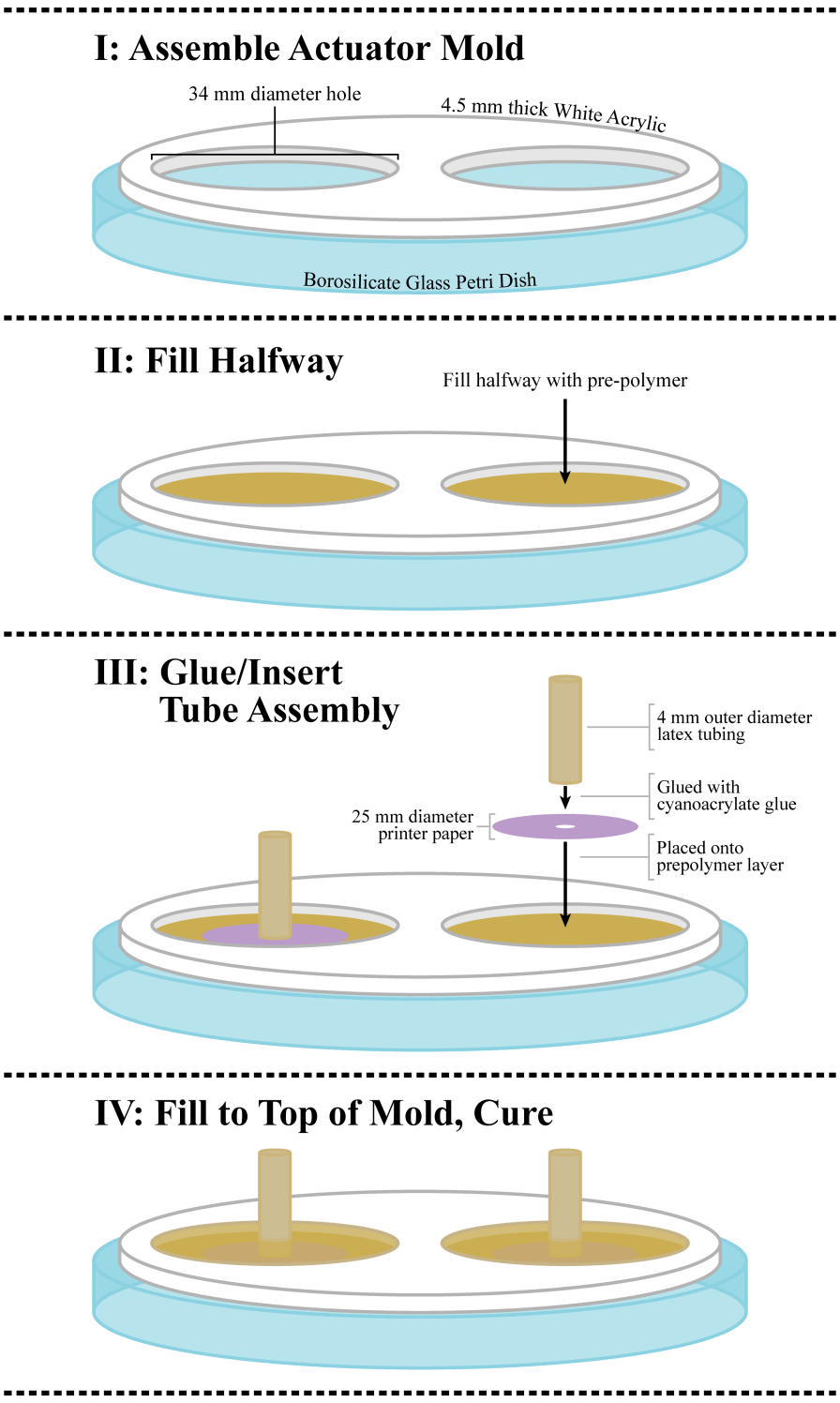

Figure 3: Assembly of a PGSI actuator by molding. A piece of printer paper is used as both a strain limiting layer and a way of creating an air pocket in the cured PGSI. The latex tubing allows for air flow into the created cavity once the actuators have been cured.

iS™ 10 spectrometer (Thermo Scientific). Resulting spectra were compared to identify differences in chemistry pre- and post-curing.

4 Results

4.1 Tensile and cyclic testing

Measured dumbbells had ultimate tensile strengths (UTS) ranging from 134 to 193 kPa, and elongations ranging from 105 to 137% at break (Figure 4-I). PGSI performed nonlinearly, and the high variance in UTS and elongation at break evidence an inconsistency in either the melt, molding, or curing processes. No correlation, however, was found between UTS or elongation at break and average melt temperature. Temperature averages compared to UTS and elongation at break include average before addition of itaconic acid (first 20 hours of melt), average after addition of itaconic acid (last 4 hours of melt), and total average (all 24 hours). No correlation was found between UTS or elongation at break and dumbbell thickness.

Due to the lack of correlation in measured melt temperatures and UTS or elongation at break, it is likely that the culprit of the observed sample strength and elasticity variance involves either the curing stage or the handling involved with molding. Temperature was not controlled during the two 30 minute curing sessions for each batch of dumbbells. Variations of temperature during this time could have caused differing levels of curing due to changes of mobility of species in the pre-polymer. Another

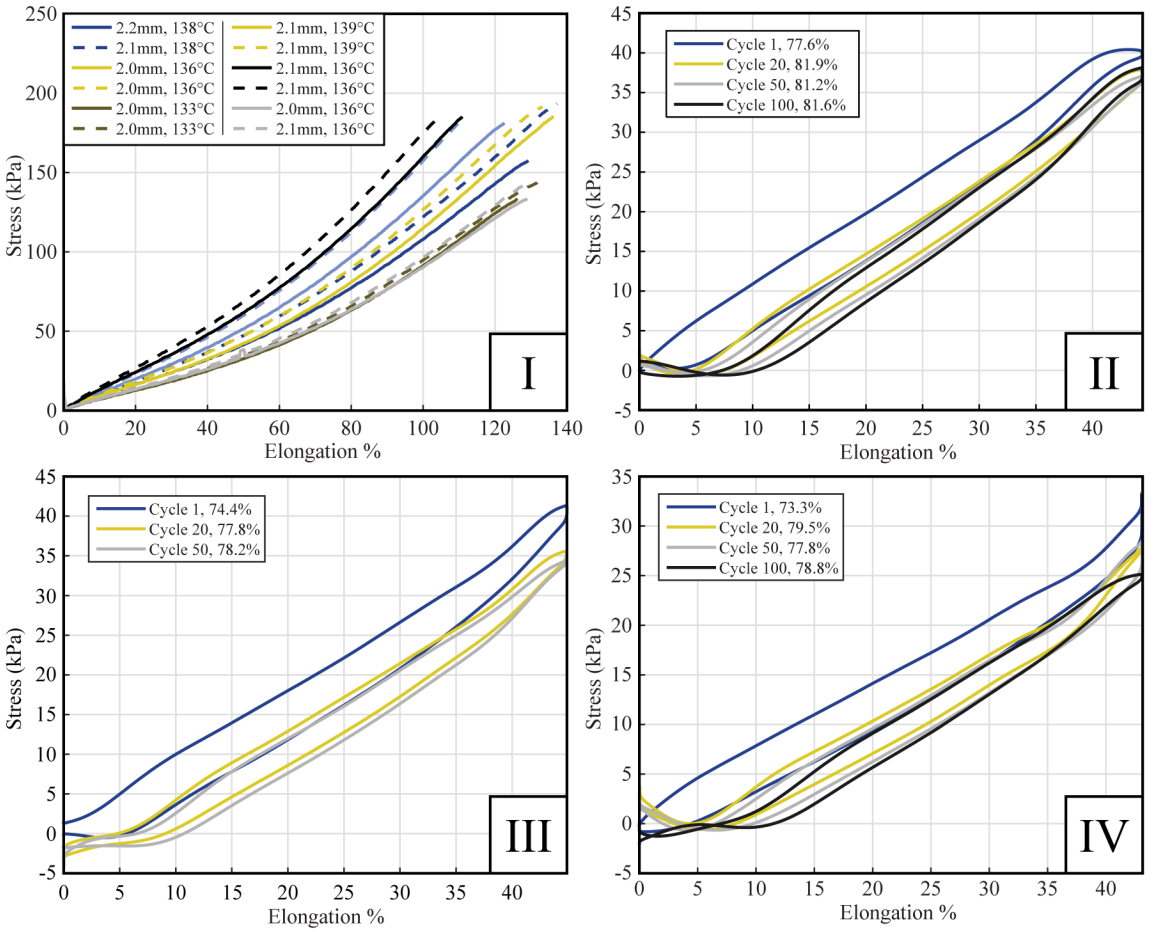

Figure 4: **I:**Tensile tests of six PGSI trials, each with two dumbbells. Trials of the same batch are the same color. All data was filtered using a moving average with a span of 5 points. Legend lists (in order): dumbbell thickness, average temperature of run. **II-IV:** Cyclic tensile tests run on dumbbells from trials run on 05/08/2017 (II), 05/14/2017 (III), and 05/16/17 (IV). Legends list (in order): cycle number, % resilience. All cyclic data was processed with a 4th degree Butterworth filter.

possible cause of the variation could be molding-induced bubbles in the dogbones, as well as scores or indents from rough or cracked mold edges.

Modulus curves of tested PGSI dumbbells are shown in Figure 5. The minimum coefficient of determination from the polynomial fits described in Section 3.4 was 0.9993, evidencing good fits. The PGSI samples were consistently stiffer than the

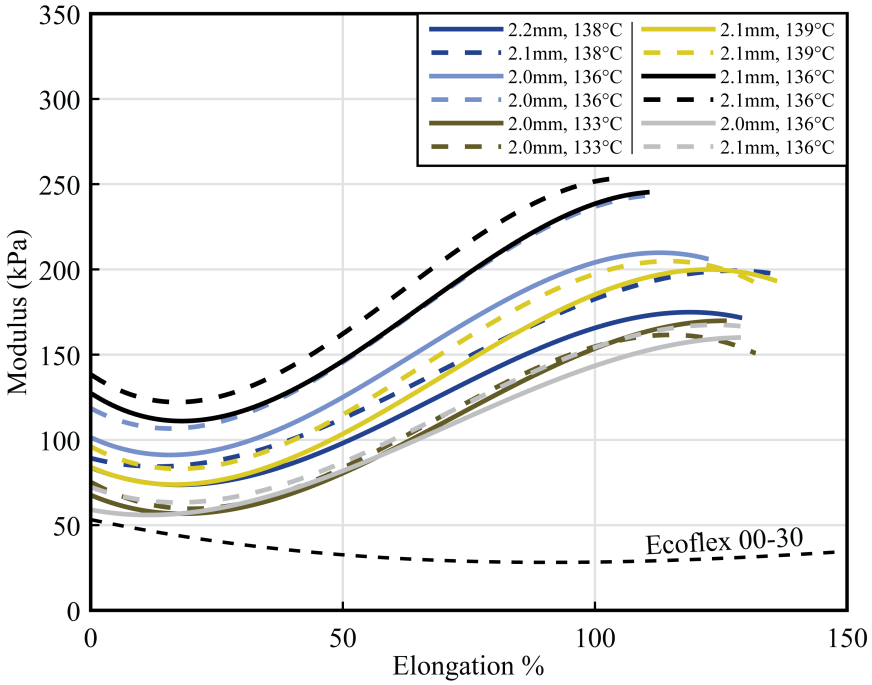

Figure 5: Modulus curves of tensile tests shown in Figure 4-I. The modulus curve of Smooth-On Ecoflex® 00-30 is superimposed on the PGSI modulus curves. Ecoflex® data used with permission from Walker et al. (2017).

tested silicone rubber, with modulus minimums ranging from 56 to 122 kPa at 11 to 22 % elongation, and modulus maximums ranging from 160 to 254 kPa at 105 to 129 % elongation. All PGSI samples showed similar modulus curve structures, with an initial dip in modulus followed by an increase, and a final dip before UTS is reached. Calculated modulus values for each PGSI sample ranged from 57 kPa to 1.31 MPa.

Age tests showed a decrease in elongation at break when dumbbells were aged at room temperature in darkness for seven days (Fig. 6). Aged samples had an observed elongation at break of 78 to 85% of the average elongation at break of the two compared fresh samples. No significant change in UTS of aged samples compared to fresh samples was seen. The aged samples maintained a similar form of nonlinearity

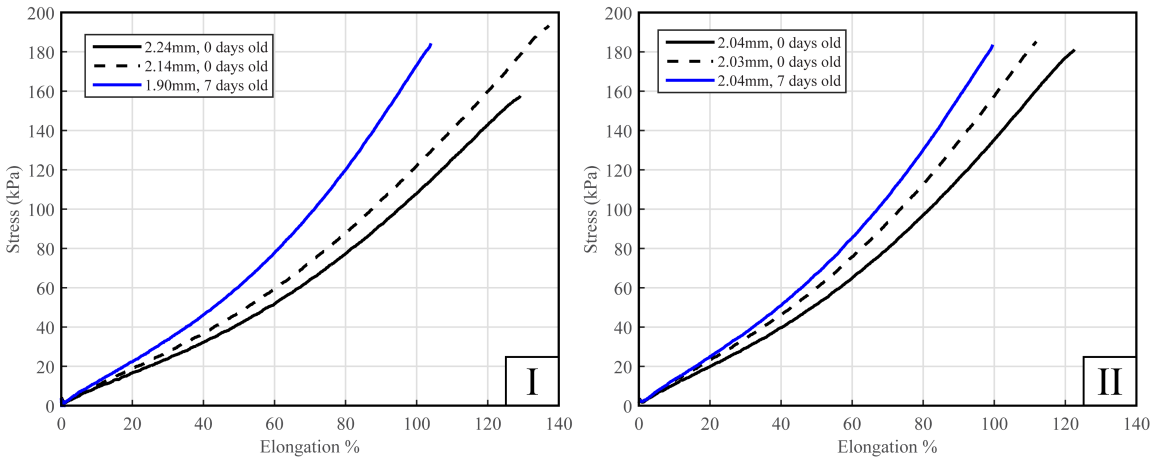

Figure 6: Tensile tests of new and aged samples from trials run on 05/08/2017 **(I)**, and 05/09/2017 **(II)**. Legends list (in order): dumbbell thickness, dumbbell age.

in their stress vs. elongation curves.

Cyclic tensile tests of three dumbbells from different trials show hysteresis, with resilience values ranging from 73 to 82%. The hysteresis suggests that the dumbbells are viscoelastic, explaining the lost energy between the loading and unloading curves. The negative stress values observed in subsequent cycles are caused by permanent deformation during the first cycle. This deformation results in buckling of the dumbbell in all cycles after the first, due to its new resting length being longer than the initial sample length. No 100th cycle is shown in Figure 4-III because the sample broke after 65 cycles.

4.2 Pocket actuator testing

Two pocket actuators were constructed via the method detailed in Section 3.5. The actuators were successfully pneumatically inflated with a syringe. The inflated ac-

Figure 7: Two PGSI pocket actuators pneumatically inflated by hand with a syringe. Both were made with a PGSI run started on 05/24/2017.

tuators are shown in Figure 7. When inflated to failure, the PGSI actuators leaked near the edge of the pocket where stress would be most concentrated.

4.3 FTIR analysis

FTIR analysis was conducted on both the uncured pre-polymer and the cured dogbone of four PGSI batches. Results between trials were extremely similar, so only one trial (from a melt run on 05/14/2017) is shown in Figure 8 for simplicity. The main visible difference between the uncured and cured spectra is the loss of a small peak at 1635 cm^{-1}. This peak aligns with the stretching vibration peak of a carbon-carbon double bond (Bruice, 2009). The decrease in peak intensity at this wavelength

from uncured to cured polymer suggests that carbon-carbon double bonds are being broken during the curing process. Since itaconic acid is the only chemical used with a methylene group, and the photoinitiator used attacks points of unsaturation via radical activation (Barrett et al., 2010), it is likely that the depleted peak seen in Figure 8 is a sign of the photoinitiator radicalizing the itaconic acid methylene groups in the process of free radical cross-linking.

The carbon-carbon double bond stretching vibration peak is considered a medium-strength peak, usually seen between 1680 and 1600 cm^{-1}. Another stretching vibration peak, that of the carbon-oxygen double bond, is in a similar range, usually seen betweeen 1780 and 1650 cm^{-1}. The carbon-oxygen double bond peak is strong, and can most likely be linked to the peak at 1750-1700 cm^{-1} adjacent to the possible carbon-carbon double bond peak (Bruice, 2009). The size distribution of these two peaks corresponds both with the historical strengths of these peaks, as well as the large number of carbonyl groups in the theorized PGSI polymer compared to methylene groups. Due to each itaconic acid and sebacic acid molecule containing two carbonyl groups, and each itaconic acid containing one methylene group, the molar ratio of carbonyl groups to methylene groups in the pre-polymer is 0.39:0.035. The order of magnitude difference in amounts of methylene and carbonyl groups is represented by peak sizes in the FTIR spectra. The carbon-oxygen double bond peak contributes to low peak separation in the area of interest, making it difficult to draw definitive conclusions on the uncured and cured structure of PGSI with FTIR alone.

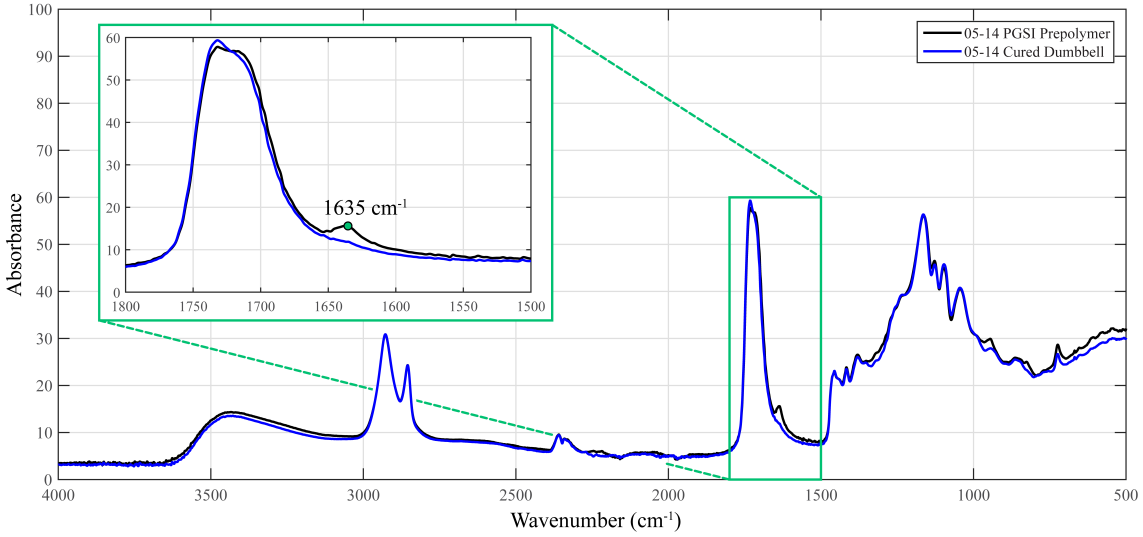

Figure 8: FTIR analysis of an uncured pre-polymer sample and a cured dumbbell sample. The most visible difference between the spectra (the peak at 1635 cm^{-1}) is labeled in the inset plot.

5 Discussion

UV-cured PGSI shows promise as a replacement for similar UV-curing biodegradable elastomers. Values of UTS and elongation at break of PGSI are comparable to the PGSA synthesized by Nijst et al. Their synthesized PGSA with degree of acrylation of 0.20 had a UTS approaching 150 kPa, and an elongation at break between 135 and 145% (Nijst et al., 2007). This is comparable to the results summarized in this paper (UTS range of 134 to 193 kPa, elongation at break range of 105 to 137%). The use of itaconic acid instead of acryloyl chloride also drastically reduces the potential hazards to those synthesizing the elastomer, as itaconic acid is much safer than acryloyl chloride (Sigma-Aldrich, 2017, 2016). Impact on the environment would also be lessened by the substitution of itaconic acid for acryloyl chloride (Barrett et al., 2010,

Tikhomirov, 1991).

PGSI also has potential applications as an SPA material. A $CaCO_3$-filled PGS was previously characterized for soft robotics, resulting in elongations at break ranging from 150 to 250% and UTS values ranging from 40 to 160 kPa (Walker et al., 2017). While elongations at break of tested PGSI samples are lower than those of the filled PGS, the calculated modulus range was within that of the filled PGS. Further adjustment of the itaconic acid to sebacic acid ratio could also tune the elongation at break and UTS of PGSI to within this range if PGSI conforms to the trends between UTS and elongation at break and degree of acrylation as shown for PGSA by Nijst et al (Nijst et al., 2007). The replacement of the 11-hour oven curing step in the PGS-$CaCO_3$ synthesis with a 1-hour UV cure is also desirable for SPA assembly due to the increased compatibility of molding and additive manufacturing methods.

The benefits of PGSI over comparable materials are significant, but so are current hurdles to expanding the technology. Molding parts out of PGSI is possible, as shown in Section 3.2, but the geometries are limited by thickness. A 1-hour cure time was required to cure 2 mm thick dumbbells, and increased time would be required for thicker parts. As thickness of samples increased, curing consistency also decreased visibly. Mold assemblies also must be resistant to the UV light and heat in the curing chamber. The chamber was observed to approach 50°C, which often led to cracking of the acrylic mold layer. This could have been caused by thermal expansion of either the acrylic material or the cyanoacrylate-based glue. These molding inconsistencies

resulted in required mold replacement after cracking and separation of the acrylic sheet from the borosilicate glass sheet caused malformations in the final molded parts.

Variations in the mold between trials could have caused inconsistency in the final tensile data (Figure 4-I). Other causes of these discrepancies include temperature variances in the melt phase (in which no direct correlation was found) causing increased or decreased PGSI chain lengths. These variations in PGSI chain lengths could affect the mobility of the radicalized photoinitiator species in the pre-polymer during the curing process. Increased chain length would result in higher viscosity, and thus lower mobility of species during curing. Decreasing viscosity of the prepolymer could therefore decrease cure times as well as increase the compatibility of the material with stereolithography. Inhomogeneity of the prepolymer with respect to polymer chain length (molecular weight), as well as frequency of itaconic acid in the polymer backbone and dispersion of photoinitiator in the mixture could also result in deviations of final material properties. The fact that two of the three cyclic tests showed the elastomer surviving all 100 cycles is promising, but the third trial breaking after 65 cycles speaks to the necessity of making the PGSI synthesis and part assembly process more consistent.

The UTS of PGSI samples aged 7 days in darkness at room temperature were comparable to that of unaged PGSI samples. This shows different trends than PGS-$CaCO_3$, which exhibited similar elongations at break but significant degradation of UTS after 8 days (Walker et al., 2017). Part of this discrepancy could be accounted

for by the use of $CaCO_3$ by Walker et al. Calcium carbonate is a weak base, which could possibly be reacting with the carboxylic functional groups of the PGS polymer chains, resulting in different aerobic degradation trends than are seen in PGSI, which has no such additive. It is important to keep in mind, as well, that PGSI samples were blocked from direct sunlight during aging. No formal tests were conducted regarding the over-curing of PGSI by the UV radiation contained in sunlight. Nonetheless, scraps of PGSI left in sunlight became less elastic and more opaque. The samples kept in darkness also showed clouding, but to a seemingly lower degree than those exposed to sunlight.

No microbial degradation testing was conducted for this material. It is likely, though, that PGSI is highly degradable due to its chemical makeup being 91% PGS by mass, which is documented as being biodegradable and even biocompatible. (Wang et al., 2002, Walker et al., 2017) Of the remaining 9%, about 8% is itaconic acid, and the rest is the photoinitiator, HCHPK. Itaconic acid has been proposed previously as a renewable feedstock for synthesizing biodegradable polymers (Barrett et al., 2010), and HCHPK is recorded to be 80% biodegradable (Sigma-Aldrich, 2014). These factors suggest that the described PGSI elastomer is highly biodegradable, but degradation testing would be required for confirmation.

6 Future work

The PGSI synthesis process would be improved by increased and more varied testing. Implementation of automated temperature control on both the melt and cure parts of the synthesis would be beneficial in pinpointing relationships between material properties and synthesis parameters. Further development efforts in making molds compatible with the curing process would also be valuable in making consistent dumbbells. Cracks and variations in the mold led to marks on the edge of the tested dumbbells, which could cause artificially low ultimate tensile strengths or premature breaking.

Trials with increased and decreased amounts of itaconic acid with respect to sebacic acid would also be valuable in adding tunability to the elastomer's mechanical properties. Nijst et al. showed a visible trend of increased elongation at break and decreased UTS with decreased degree of acrylation of PGSA, which is theoretically synonymous with ratio of itaconic acid in PGSI. Providing this range of possible material properties and their corresponding chemical recipes would allow a higher range of use within the field of soft robotics. It will also allow better comparison between PGSI and PGSA, and will help establish whether PGSI is an adequate replacement for PGSA in all formulations, or if only for a small subsection of PGSA recipes documented by Nijst et al (2007).

More thorough chemical analysis of PGSI, both uncured and cured, is required to establish the method of cross-linking. The FTIR analysis conducted provided

evidence suggesting the decrease of methylene groups during curing (Fig. 8), but the location and nature of the final cross-link is still unconfirmed. The resultant cross-link could, for example, be between methylene groups on itaconic acid incorporated into the PGS backbone, or it could be between a methylene group and another part of the PGS backbone, such as hydrogens on saturated carbons.

Comprehensive degradation tests should be conducted on PGSI in order to determine the lifespan of the elastomer, as well as its overall biodegradability. The lifespan of the elastomer could affect its possible applications in SPAs, as well as in other possible applications such as in medical implants. For the latter application, biocompatibility research would also be necessary. Analysis of the resultant chemical products of biodegradation would also be ideal, as the information could result in better understanding of possible environmental impacts of the material. This could also inform possible variations in the PGSI recipe; calcium carbonate could, for example, be considered as an additive as Walker et al. proposed, if the degradation resulted in overly acidic products.

Future work in solvents compatible with the PGSI prepolymer would also be beneficial. Finding a solvent which does not inhibit PGSI curing would help to lower the viscosity of the prepolymer, making stereolithography or other additive manufacturing techniques more accessible.

Pocket actuators were constructed out of PGSI in this work, but they were not characterized. Actuator characterization, including but not limited to the study of

expansion vs. chamber pressure, would help to verify the usability of PGSI in the field of soft robotics.

7 Conclusion

In this work we have introduced a UV-curing, biodegradable, and renewable elastomer, PGSI, and have characterized it for use in SPAs. This research was prompted by difficulties in similarly formulated thermoset materials (Walker et al., 2017), and health concerns in similarly formulated UV-curing materials (Nijst et al., 2007). Due to the relatively benign reagents used in the proposed synthesis method, researchers synthesizing PGSI will be in less danger of immediate or chronic health detriments common with chemicals often used in similar materials syntheses (Sigma-Aldrich, 2016). Soft robotics researchers would be benefited by this, as well as the simple, one-pot synthesis method and easily acquired parts and straightforward assembly of UV-curing equipment (see Sections 3.1-3.2). Future work is required in the areas of recipe deviation in hopes of establishing material property tunability. Comprehensive degradation testing must also be conducted to verify the theoretically biodegradable nature of PGSI. We hope that this project helps encourage materials scientists to look into greener, less hazardous alternatives to commonly used chemicals in hopes of protecting both the chemical worker and the environment.

8 Acknowledgements

The author thanks Dr. John Simonsen for his guidance regarding photopolymers and photocrosslinking; Dr. Yigit Menguc for his help in planning and funding; Steph Walker for her massive amounts of contributed time and support; and Dylan Sures for his equipment training and assistance.

9 Appendix

9.1 PGSI process development

The presented PGSI synthesis route and recipe was a result of many trials and iterations. The work of Walker et al. was used as a starting point (Walker et al., 2017), and itaconic acid was added to replace 20 molar percent of the existing sebacic acid. HCHPK was added such that it was 1 wt.% ratio of the final melt. Sebacic acid, itaconic acid, and glycerol were all added at the beginning of the melt, with the HCHPK added near the end. From this, a waxy, stiff polymer was formed. To increase the elasticity of the polymer, the itaconic acid was added later. This was done to allow formation of PGS chains before the itaconic acid was added into the polymer backbone, therefore spacing out the itaconic acid in the polymer. This would theoretically space out the cross-links in the resulting polymer network, allowing for increased elasticity. The resultant proposed pre-polymer structure and process is shown in Figure 9.

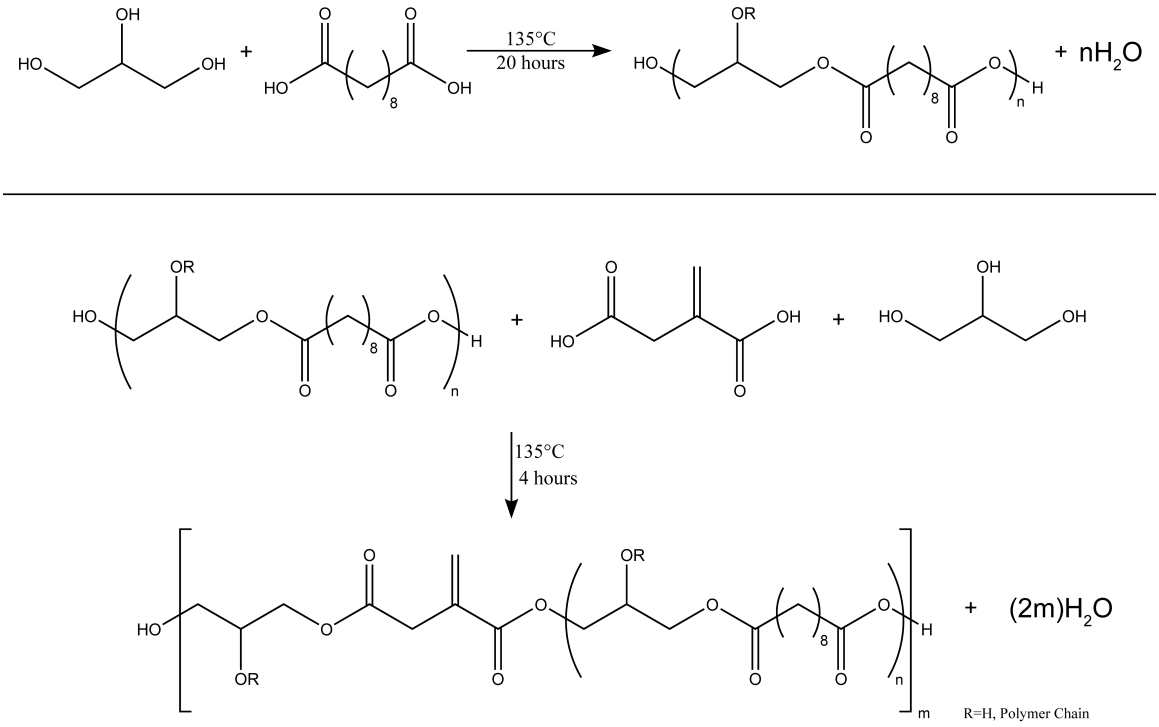

Figure 9: A proposed PGSI pre-polymer synthesis process. **Top:** a standard PGS synthesis is conducted for 20 hours. **Bottom:** the PGS chains react with glycerol (already in flask) and the added itaconic acid to form the final pre-polymer.

The UV-curing chamber described in Section 3.1 was designed with ease of assembly and adoption in mind. All materials used in the chamber assembly are easily acquired—a cardboard box, aluminum foil, antimicrobial bulbs, clear acrylic sheets. A commercial UV-curing chamber would most likely be more effective in curing the PGSI pre-polymer, due to possible higher luminosity of UV light. A commercial chamber may also have temperature control capabilities, which could decrease the variance in final PGSI mechanical properties seen in this work's results. The handmade chamber described here, however, was able to make a material with relatively consistent results, and could therefore be applicable in robotics labs that do not have

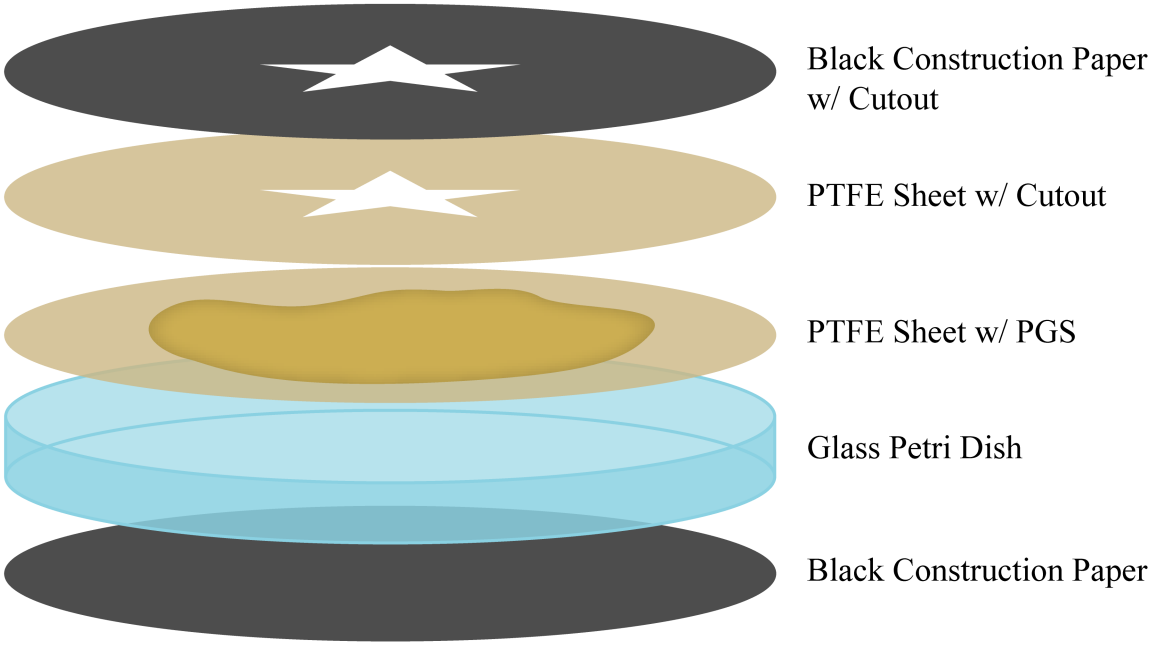

Figure 10: Expanded structure of the PGSI masking test assembly. PTFE sheets were used as nonstick layers, and black construction paper was used to block UV light—in its entirety from below, and in all but the desired final shape's area from above.

access to or funds for a more elaborate UV-curing setup.

9.2 Supplemental testing

Multiple tests were performed on PGSI before and during scale-up to help verify our theories on curing. One such test was a masking test, which aimed to test the viability of PGSI as a stereolithography bath material (assuming it would first be thinned via filler or solvent). The setup for this test is shown in Figure 10, and the resultant star-shaped PGSI sample is shown in Figure 11.

The masking test also served as a way to find out if any of the curing was coming from incident heat. The UV curing chamber could get up to about 50°C, which

Figure 11: Cured PGSI star resultant from the curing method shown in Figure 10.

raised concerns about whether the PGSI was curing from the UV light emitted from the bulbs, or from the resultant heat. When the masking trial was conducted, the masked sections of pre-polymer were only exposed to the incident heat, and they did not cure. This let us conclude that the PGSI was not curing from heat alone, and that the UV exposure played an important role in curing.

10 References

Agarwal, G., Besuchet, N., Audergon, B., and Paik, J. (2016). Stretchable Materials for Robust Soft Actuators towards Assistive Wearable Devices. *Scientific Reports*,

6:34224.

Anastas, P. and Eghbali, N. (2009). Green Chemistry: Principles and Practice. *Chemical Society Reviews*, 39(1):301–312.

ASTM International (2016). Standard Test Methods for Vulcanized Rubber and Thermoplastic Elastomers—Tension. Technical report, ASTM International.

Barrett, D. G., Merkel, T. J., Luft, J. C., and Yousaf, M. N. (2010). One-Step Syntheses of Photocurable Polyesters Based on a Renewable Resource. *Macromolecules*, 43(23):9660–9667.

Bellingham, C. M., Lillie, M. A., Gosline, J. M., Wright, G. M., Starcher, B. C., Bailey, A. J., Woodhouse, K. A., and Keeley, F. W. (2003). Recombinant human elastin polypeptides self-assemble into biomaterials with elastin-like properties. *Biopolymers*, 70(4):445–455.

Bruice, P. Y. (2009). *Organic Chemistry, 6th Edition*. Prentice Hall, 6 edition edition.

Cho, K.-J., Koh, J.-S., Kim, S., Chu, W.-S., Hong, Y., and Ahn, S.-H. (2009). Review of manufacturing processes for soft biomimetic robots. *International Journal of Precision Engineering and Manufacturing*, 10(3):171–181.

Ciba Specialty Chemicals (2001). Ciba® IRGACURE® 184. Technical report.

Colas, A. and Aguadisch, L. (1997). Silicones in pharmaceutical applications. *Chimie Nouvelle*, 15(58):1779.

Connolly, F., Polygerinos, P., Walsh, C. J., and Bertoldi, K. (2015). Mechanical Programming of Soft Actuators by Varying Fiber Angle. *Soft Robotics*, 2(1):26–32.

Daemi, H., Rajabi-Zeleti, S., Sardon, H., Barikani, M., Khademhosseini, A., and Baharvand, H. (2016). A robust super-tough biodegradable elastomer engineered by supramolecular ionic interactions. *Biomaterials*, 84:54–63.

Dodiuk, H. and Goodman, S. H. (2014). 1 - Introduction. In *Handbook of Thermoset Plastics (Third Edition)*, pages 1–12. William Andrew Publishing, Boston. DOI: 10.1016/B978-1-4557-3107-7.00001-4.

Dow Corning (2016). The 2015 Corporate Sustainability Report. Technical report, Dow Corning.

Formlabs (2017). Form 2 Desktop SLA 3d Printer.

Fouassier, J. P. and Lalevée, J. (2012). Basic Principles and Applications of Photopolymerization Reactions. In *Photoinitiators for Polymer Synthesis*, pages 1–1. Wiley-VCH Verlag GmbH & Co. KGaA. DOI: 10.1002/9783527648245.part1.

Godaba, H., Li, J., Wang, Y., and Zhu, J. (2016). A Soft Jellyfish Robot Driven by a Dielectric Elastomer Actuator. *IEEE Robotics and Automation Letters*, 1(2):624–631.

Green, W. A. (2010). *Industrial Photoinitiators*. CRC Press, 1 edition.

Greene, J. (2014). *Sustainable Plastics*. John Wiley & Sons, Incorporated, 1 edition.

Ilievski, F., Mazzeo, A. D., Shepherd, R. F., Chen, X., and Whitesides, G. M. (2011). Soft Robotics for Chemists. *Angewandte Chemie International Edition*, 50(8):1890–1895.

Laschi, C., Cianchetti, M., Mazzolai, B., Margheri, L., Follador, M., and Dario, P. (2012). Soft Robot Arm Inspired by the Octopus. *Advanced Robotics*, 26(7):709–727.

Leon-Rodriguez, H., Le, V. H., Ko, S. Y., Park, J. O., and Park, S. (2015). Ferrofluid soft-robot bio-inspired by Amoeba locomotion. In *2015 15th International Conference on Control, Automation and Systems (ICCAS)*, pages 1833–1838.

Li, X., Shi, J., Wu, K., Luo, F., Zhang, S., Guan, X., and Lu, M. (2017). A novel pH-sensitive aqueous supramolecular structured photoinitiator comprising of 6-modified per-methylated β-cyclodextrin and 1-hydroxycyclohexyl phenyl ketone. *Journal of Photochemistry and Photobiology A: Chemistry*, 333:18–25.

Lorenz, G. and Kandelbauer, A. (2014). 14 - Silicones. In *Handbook of Thermoset Plastics (Third Edition)*, pages 555–575. William Andrew Publishing, Boston. DOI: 10.1016/B978-1-4557-3107-7.00014-2.

Lukasiak, J., Dorosz, A., Prokopowicz, M., Rosciszewski, P., and Falkiewicz, B. (2005). Biodegradation of silicones (organosiloxanes). *Biopolymers Online*.

Magalhães, A. I., Carvalho, J. C. d., Medina, J. D. C., and Soccol, C. R. (2017).

Downstream process development in biotechnological itaconic acid manufacturing. *Applied Microbiology and Biotechnology*, 101(1):1–12.

Miyashita, S., Guitron, S., Ludersdorfer, M., Sung, C., and Rus, D. (2015). An untethered miniature origami robot that self-folds, walks, swims, and degrades. In *2015 IEEE International Conference on Robotics and Automation (ICRA)*, pages 1490–1496.

Mosadegh, B., Polygerinos, P., Keplinger, C., Wennstedt, S., Shepherd, R. F., Gupta, U., Shim, J., Bertoldi, K., Walsh, C. J., and Whitesides, G. M. (2014). Pneumatic Networks for Soft Robotics that Actuate Rapidly. *Advanced Functional Materials*, 24(15):2163–2170.

Moseley, P., Florez, J. M., Sonar, H. A., Agarwal, G., Curtin, W., and Paik, J. (2016). Modeling, Design, and Development of Soft Pneumatic Actuators with Finite Element Method. *Advanced Engineering Materials*, 18(6):978–988.

Mucci, V. and Vallo, C. (2012). Efficiency of 2,2-dimethoxy-2-phenylacetophenone for the photopolymerization of methacrylate monomers in thick sections. *Journal of Applied Polymer Science*, 123(1):418–425.

Nijst, C. L. E., Bruggeman, J. P., Karp, J. M., Ferreira, L., Zumbuehl, A., Bettinger, C. J., and Langer, R. (2007). Synthesis and Characterization of Photocurable Elastomers from Poly(glycerol-co-sebacate). *Biomacromolecules*, 8(10):3067–3073.

QVF Group (2007). QVF Group Components Catalog.

Ratna, D. (2009). *Handbook of Thermoset Resins*. iSmithers Rapra Publishing, Shrewsbury.

Rus, D. and Tolley, M. T. (2015). Design, fabrication and control of soft robots. *Nature*, 521(7553):467–475.

Seok, S., Onal, C. D., Cho, K. J., Wood, R. J., Rus, D., and Kim, S. (2013). Meshworm: A Peristaltic Soft Robot With Antagonistic Nickel Titanium Coil Actuators. *IEEE/ASME Transactions on Mechatronics*, 18(5):1485–1497.

Shian, S., Bertoldi, K., and Clarke, D. R. (2015). Dielectric Elastomer Based "Grippers" for Soft Robotics. *Advanced Materials*, 27(43):6814–6819.

Sigma-Aldrich (2014). 1-hydroxycyclohexyl phenyl ketone. Safety Data Sheet, Sigma-Aldrich.

Sigma-Aldrich (2016). Acryloyl Chloride. Safety Data Sheet, Sigma-Aldrich.

Sigma-Aldrich (2017). Itaconic Acid. Safety Data Sheet, Sigma-Aldrich.

Stratasys (2017). PolyJet Technology.

Tikhomirov, I. P. (1991). Effect of acrylate industry wastes on the environment and the prevention of their harmful action. *Vestnik Akademii meditsinskikh nauk SSSR*, (2):21–25.

Walker, S., Rueben, J., Volkenburg, T. V., Hemleben, S., Grimm, C., Simonsen, J., and Mengüç, Y. (2017). Using an environmentally benign and degradable elastomer

in soft robotics. *International Journal of Intelligent Robotics and Applications*, pages 1–19.

Wang, Y., Ameer, G. A., Sheppard, B. J., and Langer, R. (2002). A tough biodegradable elastomer. *Nature Biotechnology*, 20(6):602–606.

Yang, J., Webb, A. R., and Ameer, G. A. (2004). Novel Citric Acid-Based Biodegradable Elastomers for Tissue Engineering. *Advanced Materials*, 16(6):511–516.

Zhao, X., Wu, Y., Du, Y., Chen, X., Lei, B., Xue, Y., and Ma, P. X. (2015). A highly bioactive and biodegradable poly(glycerol sebacate)–silica glass hybrid elastomer with tailored mechanical properties for bone tissue regeneration. *Journal of Materials Chemistry B*, 3(16):3222–3233.